ChemComm

COMMUNICATION

View Article Online
View Journal

Cite this: DOI: 10.1039/c5cc03943f

Received 12th May 2015,
Accepted 27th May 2015

DOI: 10.1039/c5cc03943f

www.rsc.org/chemcomm

Room-temperature acetylene hydration by a Hg(II)-laced metal–organic framework†‡

Ka-Kit Yee,[a] Yan-Lung Wong,[a] Meiqin Zha,[a] Ramesh Y. Adhikari,[b] Mark T. Tuominen,[b] Jun He[c] and Zhengtao Xu*[a]

Thiol (–SH) groups within a Zr(IV)-based metal–organic framework (MOF) anchor Hg(II) atoms; oxidation by H_2O_2 then leads to acidic sulfonate functions for catalyzing acetylene hydration at room temperature.

Among the various ways to functionalize the porous solids of metal–organic frameworks (MOFs),[1] the versatile reactivity of the thiol (–SH) group offers unique advantages.[2] For example, thiols as strong soft donors readily take up various metal ions, which closely bears on the removal of heavy metal ions,[3] and on the creation of electroactive/semiconducting[2b,4] or catalytic sites[5] (*e.g.*, mimicking the iron–sulfur, copper–sulfur proteins) within the MOF matrices. Notably, recent exercises (*e.g.*, using 2,5-dimercapto-1,4-benzenedicarboxylic acid, H_2DMBD, Chart 1) indicated that dense arrays of free-standing thiol groups can be built into the host net when chemically very hard ions [like Eu(III), Zr(IV) or Al(IV); *i.e.*, these tend to stay unbonded with the thiol group] are chosen to link the carboxyl groups.[3a,5c]

As part of our ongoing efforts to further exploit the thiol/thiolate groups thus installed within MOF solids, we utilize here simple oxidation to effect the conversion into sulfonic acid and metal sulfonate functions.[6] Such conversion is intended to liberate the proton and metal centers from the thiol groups, and to create strong acidity and reactivity properties within the MOF pores.

One major advantage of this method lies in the dense array of sulfonate units that can be installed (*e.g.*, two per linker, as from DMBD). Previously, MOF systems (*e.g.*, MIL-101(Cr), MIL-53(Al)[7] and others[8]) had been directly sulfated (*e.g.*, by $ClSO_3H$); but the sulfonate group, once attached, deactivated the aromatic core and thus hindered further sulfation (*i.e.*, the number of installed sulfonate is limited). In another approach, sulfated ligands and pristine ligands as a mixture were reacted directly with metal ions to form the framework, but potential interference from the sulfonate group for binding with the metal ions (and thus disrupting the network construction) often limits the fraction of the sulfonated ligands. More broadly, the oxidation of the metal thiolate moiety generates *in situ* metal sulfonate functions on the host net, whereas for other sulfated frameworks, additional steps of ion exchange are necessary for inserting exo-framework metal ions.[9] As thiol groups readily bind various metal ions, our approach offers flexible control over the amount and type of metal ions to be deployed in the pores. For illustration, we present here a MOF solid with Hg^{2+}-sulfonate functions as an especially active catalyst for the acetylene hydration reaction.

First we introduce the three major stages of sample preparation. (1) Reaction of $ZrCl_4$ and H_2DMBD under solvothermal conditions yielded a crystalline powder sample of the thiol-laced ZrDMBD framework (a similar procedure to that reported,[3a] but with N_2 protection to minimize the oxidation of the –SH groups). The composition of the ZrDMBD sample features a $Zr_6O_4(OH)_4$·$(DMBD)_6$ framework with DMF and H_2O guests (see the ESI‡ for details; see also Fig. 1, left for a schematic of the framework). (2) Treatment of ZrDMBD with an aqueous solution of $HgCl_2$ led to the mercurated solid ZrDMBD-Hg, which was found to contain a 1 : 6 : 4 $Zr_6O_4(OH)_4$/DMBD/Hg ratio (together with Cl^-, DMF and H_2O; equivalent to w/w 21.4% for Hg; see the ESI‡ for details).

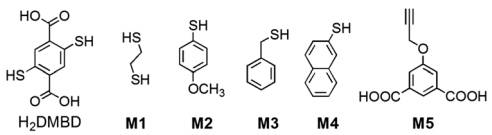

Chart 1 Molecule H_2DMBD for building the ZrDMBD solid, **M1–M4** for the selective uptake test with the ZrBDSO$_3$-Hg solid, and **M5** for a hydration test benchmarked against acetylene.

[a] *Department of Biology and Chemistry, City University of Hong Kong, 83 Tat Chee Avenue, Kowloon, Hong Kong, China. E-mail: zhengtao@cityu.edu.hk*
[b] *Department of Physics, University of Massachusetts, Amherst, Massachusetts 01003, USA*
[c] *School of Chemical Engineering and Light Industry, University of Technology, Guangzhou 510006, Guangdong, China*

† Dedicated to the 60th birthday of Prof. Stephen Lee.

‡ Electronic supplementary information (ESI) available: Experimental procedures; network synthesis and activation; SEM photographs; elemental analysis, CO_2 sorption, TGA, IR/Raman, and PXRD data. See DOI: 10.1039/c5cc03943f

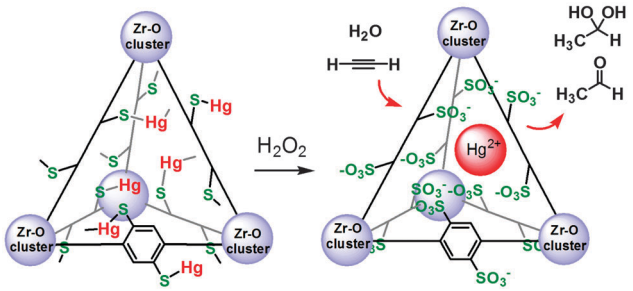

Fig. 1 Schematics for H_2O_2 oxidation of the ZrDMBD-Hg net (left) into the $ZrBDSO_3$-Hg net (right) and the use of the latter in catalysing the hydration of acetylene. The host net is simplified as a tetrahedral cage, with each $Zr_6O_4(OH)_4$ cluster shown as purple spheres.

The substantial Hg presence in ZrDMBD-Hg was also revealed by the absence of S–H in the IR/Raman spectra (Fig. S1 and S2, ESI‡), as well as the large change in the intensity profile of the PXRD patterns (*cf.* patterns b and c in Fig. 2). (3) Oxidation by H_2O_2 on ZrDMBD-Hg converts the thiolate groups into sulfonate functions; the resultant solid (denoted as $ZrBDSO_3$-Hg) was found by elemental analyses (see ESI‡) to feature the composition, $Zr_6O_4(OH)_4{\cdot}[C_8H_2O_4(SO_3^-)_{0.8}(SO_3H)_{1.2}]_6{\cdot}Hg_{2.4}{\cdot}(H_2O)_{50}$, with the formation of the sulfonate functions ($-SO_3^-$) being indicated by the IR (Fig. S1, ESI‡) and NMR spectra (Fig. S3, ESI‡). In spite of the drastic oxidative transformation, the structural integrity of the host net was found by PXRD to be intact (Fig. 2, pattern d). Compared with the ZrDMBD-Hg sample, the Hg content in $ZrBDSO_3$-Hg (11.8%) is lower, *i.e.*, about 40% of the Hg leached away during the H_2O_2 treatment; however, such Hg(II) leaching from the solid host can be readily suppressed by using a H_2O_2 solution containing dissolved $Hg(NO_3)_2$, *e.g.*, with the resultant Hg content being 20.4% (see SI for the procedure and PXRD pattern g in Fig. S4, ESI‡). For the following catalytic study, the $ZrBDSO_3$-Hg sample (*i.e.*, with a 6 : 2.4 linker/Hg ratio) was prepared by the simple H_2O_2 treatment—without the addition of $Hg(NO_3)_2$ solute.

Can one use ion exchange (*i.e.*, with $ZrBDSO_3H$) instead to access the $ZrBDSO_3$-Hg solid? To explore this possibility, the thiol groups in ZrDMBD were oxidized by H_2O_2 into sulfonic acid groups—see the ESI‡ for the procedure and characterization (Fig. S1–S4, ESI‡) of the resultant $ZrBDSO_3H$ solid, and for the measured proton conductivity (Fig. S5, ESI;‡ the conductivity can be improved by H_2SO_4 treatment on the powder sample, as shown in a recent study[6]). Notably, ion exchange experiments on the $ZrBDSO_3H$ solid thus obtained indicated less Hg^{2+} insertion. For example, even after the $ZrBDSO_3H$ solid was heated in concentrated $Hg(NO_3)_2$ and $HgCl_2$ solutions for 18 hours (ESI,‡ for the procedures and patterns d and e in Fig. S4), the Hg content in the solid was found by the diphenylthiocarbazone extraction method analysis to be 2.8% and 3.0% (significantly lower than the values of 11.8–20.4% in the $ZrBDSO_3$-Hg samples obtained from H_2O_2 oxidation on ZrDMBD-Hg). Such tests help to highlight ZrDMBD-Hg as an effective precursor to highly mercurated $ZrBDSO_3$-Hg products.

An additional test also helps to demonstrate that the Hg^{2+} ions are located inside of the $ZrBDSO_3$-Hg pores. Specifically, a mixture solution of four mercaptan molecules (in CD_2Cl_2; **M1–M4** are shown in Chart 1) of increasing sizes was treated by $ZrBDSO_3$-Hg (containing Hg in excess relative to the thiols) at room temperature (rt). While NMR measurement indicated complete removal of the smallest **M1** (*via* the strong thiol-Hg interaction) from the solution within 12 h, the concentrations of the larger **M2**, **M3** and **M4** remained unchanged (Fig. S6, ESI‡). Such size selectivity indicates that the Hg^{2+} ions are not accessible to the larger **M2–M4** mercaptans under these conditions, and points to potential applications in thiol uptake (see also Fig. S7, ESI‡ for the sorption test on 2-mercaptoethanol).

The catalytic efficacy of the $ZrBDSO_3$-Hg solid towards acetylene hydration of (C_2H_2) was revealed in a simple reaction setup. Namely, by stirring at rt for a few hours a mixture of the $ZrBDSO_3$-Hg solid (*e.g.*, 100 mg, containing 0.059 mmol of Hg) and water (*e.g.*, 2.7 mL; 0.15 mol) in a 1000 mL Schlenk flask filled with acetylene (C_2H_2; atmospheric pressure; about 45 mmol, 1.2 g), an acetaldehyde content (in the form of acetaldehyde and the hydration product ethane-1,1-diol; Fig. 1) of 5.78% (equivalent to a turnover number of 61 for Hg, Table 1) can be achieved in the water phase (supernatant; see Fig. 3 for the NMR spectrum). The product concentration compares well with the values (about 2–7%) normally obtained in industrial reactor settings using the homogeneous catalyst of

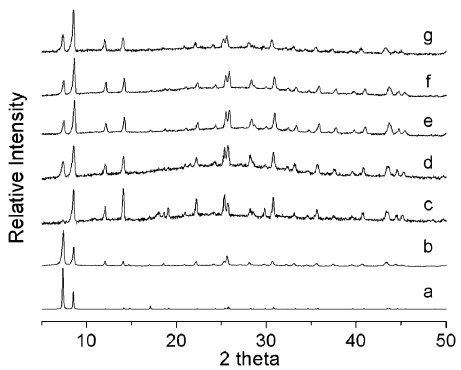

Fig. 2 X-ray powder patterns (Cu Kα = 1.5418 Å) of (a) a simulation from a structure model of ZrDMBD; (b) an as-made ZrDMBD sample; (c) ZrDMBD-Hg; (d) $ZrBDSO_3$-Hg; (e–g) $ZrBDSO_3$-Hg after the 1st, 2nd and 3rd cycle of the acetylene hydration catalysis test, respectively.

Table 1 Efficiencies of $ZrBDSO_3$-Hg as a Lewis acid for hydration of acetylene

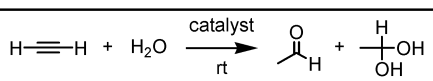

Catalyst	Hg content in MOF (wt%)	Total Hg (mg)	Product conc. (wt%)	TON[b]
$ZrBDSO_3$-Hg cycle 1	11.8[a]	11.8	5.78	61
$ZrBDSO_3$-Hg cycle 2[c]	11.9[a]	8.3	5.95	62
$ZrBDSO_3$-Hg cycle 3[c]	11.4[a]	6.9	5.68	59
$HgSO_4/H_2SO_4$	N/A	12.3	1.14	13

[a] Mercury contents were determined using the diphenylthiocarbazone extraction method. [b] TON is defined as the number of products formed per mercury atom. [c] See the ESI or the cycling procedure.

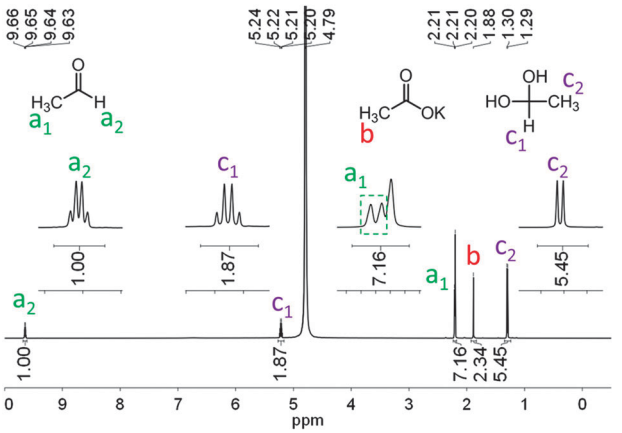

Fig. 3 ^{1}H NMR spectrum of the supernatant of acetylene reaction (dissolved in D_2O with CH_3COOK added as an internal standard). The internal standard peak at 1.88 ppm (singlet) and the product peak at 9.65 ppm (quartet) from acetaldehyde and 1.30 ppm (doublet) from ethane-1,1-diol were used to calculate the yield and TON.

$HgSO_4/H_2SO_4$ solutions,[10] which nevertheless involve the more sophisticated conditions of constant flow of C_2H_2 and significant heating (at 70–90 °C). As a solid state catalyst, $ZrBDSO_3$-Hg, with both the H^+ and Hg^{2+} agents lodged within its host net, provides the added advantages of non-corrosive (*e.g.*, water) conditions and easy product isolation. Such advantages stand out even in comparison with the mainstream Wacker process,[11] wherein the highly oxidizing and corrosive nature of the aqueous $PdCl_2/CuCl_2$ catalyst (aggravated under the heated conditions) remains a concern.

For a more direct benchmark, a homogeneous catalyst consisting of $HgSO_4$ (18.2 mg, 0.061 mmol) dissolved in H_2SO_4 (18%, 2.7 mL) was examined under the same reaction conditions (*e.g.*, 1.0 atm of C_2H_2, rt). Notice that both the Hg quantity and the solution volume are set to the same values as in the above test of the $ZrBDSO_3$-Hg solid. In this homogeneous setting, the acetaldehyde products amounted to only 1.14% (TON: 12.8) in the solution, less than 1/5 of the value achieved by the $ZrBDSO_3$-Hg solid catalyst. The efficiency of the $ZrBDSO_3$-Hg solid catalyst can be ascribed to the compact arrangement of the H^+ and Hg^{2+} agents within the host net, as well as to the hydrophobic aromatic struts promoting the C_2H_2 diffusion into the pores.

Also notably, the leaching of Hg(II) from the $ZrBDSO_3$-Hg solid into the water phase (supernatant) is small: *e.g.*, the supernatant (*i.e.*, 2.7 mL) was found to contain only 0.11 mg of mercury (equivalent to 40.7 ppm). In other words, less than 1% of the Hg content (11.8 mg) in the $ZrBDSO_3$-Hg catalyst was leached into the water phase during the C_2H_2 hydration process. The small Hg leaching, besides minimizing the environmental impact from the toxic Hg species, also makes it possible to recover the solid state catalyst for subsequent cycles of reactions—*e.g.*, reducing the need for re-inserting Hg^{2+} ions into the solid host.

The recovery involves oxidation (back into Hg^{2+}) of the reduced Hg species resulting from side reactions. In the traditional homogeneous $HgSO_4/H_2SO_4$ systems, such side reactions were severe, forming a large amount of Hg(0)/Hg(I)-containing sludge that had to be periodically drained from the industrial reactor. In the case of $ZrBDSO_3$-Hg, as an indication of the ongoing reduction of Hg(II) ions, the white catalyst solid gradually developed a grey color, with a concomitant decrease in catalytic activity. The used $ZrBDSO_3$-Hg solid can be reactivated simply by immersion in a mixed solution of H_2O_2, HNO_3, and $Hg(NO_3)_2{\cdot}H_2O$ at rt (*e.g.*, for 15 minutes; see the ESI‡ for details). The color of the solid returned to white, and the Hg content in the regenerated $ZrBDSO_3$-Hg solid was found to be 11.9% (*cf.* 10.0% in the used catalyst), indicating the efficacy of the solid host in retaining the Hg(II) guests. The $ZrBDSO_3$-Hg catalyst thus regenerated retains the structural integrity of the host lattice (*e.g.*, see PXRD patterns e–g in Fig. 2) and continues to be highly active for C_2H_2 hydration, with turnover numbers (*e.g.*, about 62) comparable to the first round (see Table 1).

To demonstrate that the catalysis takes places within the pores of the $ZrBDSO_3$-Hg solid, we examine the reactivity of a larger substrate, 5-propargyloxyisophthalic acid (**M5**), which, with a cross-section above 7 Å, is too bulky to enter into the host net (pore opening ~5 Å). To promote the solubility, a 2 : 1 THF/H_2O solvent was used for the hydration reaction. No reaction was observed after stirring a mixture of the $ZrBDSO_3$-Hg solid and the THF/H_2O solution of **M5** at rt for up to 8 hours (see the ESI‡ for details including NMR and TLC monitoring, *e.g.*, Fig. S8 and S9, ESI‡); by contrast, when the homogeneous system of $HgSO_4/H_2SO_4$ was used instead, the homogeneous conditions led to complete hydration of **M5** (*e.g.*, also at rt and within 8 h; see the NMR spectrum C of Fig. S8, ESI‡). This observation suggests that catalytic activity of $ZrBDSO_3$-Hg entails substrates penetrating the host net, and the Hg^{2+} ions operate from within the pores of the host net.

To sum up, the thiol function in ZrDMBD proves especially useful for accessing the Hg^{2+}-laden solid of $ZrBDSO_3$-Hg. The mild conditions (at rt, in water) for C_2H_2 hydration attest to the enhanced activity of $ZrBDSO_3$-Hg as a solid state catalyst. The catalytic activity likely results from the conjoint working of the Hg^{2+} and $-SO_3H$ acid units that are densely arrayed within the pores of the host net—*e.g.*, neither ZrBMBD-Hg nor $ZrBDSO_3H$ exhibited observable catalytic activity under similar conditions (Fig. S14, ESI‡). We are working to access similar MOF materials with larger pores, in order to widen the scope of alkyne hydration applications.[12] Imbedding metal ions in porous frameworks offers great potential for opening novel reactivities, and thiol-laced frameworks will remain uniquely important in these studies.

This work was supported by the City University of Hong Kong (Project 9667092), the Research Grants Council of HKSAR (GRF Project 103212) and the National Natural Science Foundation of China (21471037, 21201042).

Notes and references

1 (*a*) K. Manna, T. Zhang, F. X. Greene and W. Lin, *J. Am. Chem. Soc.*, 2015, **137**, 2665; (*b*) S. Yuan, W. Lu, Y.-P. Chen, Q. Zhang, T.-F. Liu, D. Feng, X. Wang, J. Qin and H.-C. Zhou, *J. Am. Chem. Soc.*, 2015,

137, 3177; (*c*) J. Jiang, F. Gandara, Y.-B. Zhang, K. Na, O. M. Yaghi and W. G. Klemperer, *J. Am. Chem. Soc.*, 2014, **136**, 12844; (*d*) J. M. Falkowski, T. Sawano, T. Zhang, G. Tsun, Y. Chen, J. V. Lockard and W. Lin, *J. Am. Chem. Soc.*, 2014, **136**, 5213; (*e*) H. J. Jeon, R. Matsuda, P. Kanoo, H. Kajiro, L. Li, H. Sato, Y. Zheng and S. Kitagawa, *Chem. Commun.*, 2014, **50**, 10861; (*f*) M. Inukai, S. Horike, W. Chen, D. Umeyama, T. Itakura and S. Kitagawa, *J. Mater. Chem. A*, 2014, **2**, 10404; (*g*) J. Cui, Y.-L. Wong, M. Zeller, A. D. Hunter and Z. Xu, *Angew. Chem., Int. Ed.*, 2014, **53**, 14438; (*h*) D. T. Genna, A. G. Wong-Foy, A. J. Matzger and M. S. Sanford, *J. Am. Chem. Soc.*, 2013, **135**, 10586; (*i*) J. M. Taylor, K. W. Dawson and G. K. H. Shimizu, *J. Am. Chem. Soc.*, 2013, **135**, 1193; (*j*) M. Yoon, K. Suh, S. Natarajan and K. Kim, *Angew. Chem., Int. Ed.*, 2013, **52**, 2688; (*k*) Z. Xu, *Coord. Chem. Rev.*, 2006, **250**, 2745; (*l*) O. M. Yaghi, G. M. Li and H. L. Li, *Nature*, 1995, **378**, 703; (*m*) G. B. Gardner, D. Venkataraman, J. S. Moore and S. Lee, *Nature*, 1995, **374**, 792; (*n*) B. F. Hoskins and R. Robson, *J. Am. Chem. Soc.*, 1989, **111**, 5962.

2 (*a*) J. He, C. Yang, Z. Xu, M. Zeller, A. D. Hunter and J. Lin, *J. Solid State Chem.*, 2009, **182**, 1821; (*b*) Z. Xu, *Metal–Organic Frameworks: Semiconducting Frameworks*, John Wiley & Sons, Ltd, Chichester, 2014.

3 (*a*) K.-K. Yee, N. Reimer, J. Liu, S.-Y. Cheng, S.-M. Yiu, J. Weber, N. Stock and Z. Xu, *J. Am. Chem. Soc.*, 2013, **135**, 7795; (*b*) B. Li, Y. Zhang, D. Ma, Z. Shi and S. Ma, *Nat. Commun.*, 2014, **5**, 5537.

4 (*a*) L. Sun, T. Miyakai, S. Seki and M. Dincă, *J. Am. Chem. Soc.*, 2013, **135**, 8185; (*b*) J. Cui and Z. Xu, *Chem. Commun.*, 2014, **50**, 3986; (*c*) D. L. Turner, T. P. Vaid, P. W. Stephens, K. H. Stone, A. G. DiPasquale and A. L. Rheingold, *J. Am. Chem. Soc.*, 2008, **130**, 14.

5 (*a*) S. Pullen, H. Fei, A. Orthaber, S. M. Cohen and S. Ott, *J. Am. Chem. Soc.*, 2013, **135**, 16997; (*b*) H. Fei and S. M. Cohen, *J. Am. Chem. Soc.*, 2015, **137**, 2191; (*c*) B. Gui, K.-K. Yee, Y.-L. Wong, S.-M. Yiu, M. Zeller, C. Wang and Z. Xu, *Chem. Commun.*, 2015, **51**, 6917.

6 W. J. Phang, H. Jo, W. R. Lee, J. H. Song, K. Yoo, B. S. Kim and C. S. Hong, *Angew. Chem., Int. Ed.*, 2015, **54**, 5142–5146.

7 M. G. Goesten, J. Juan-Alcaniz, E. V. Ramos-Fernandez, K. B. S. S. Gupta, E. Stavitski, H. van Bekkum, J. Gascon and F. Kapteijn, *J. Catal.*, 2011, **281**, 177.

8 (*a*) S. Biswas, J. Zhang, Z. Li, Y.-Y. Liu, M. Grzywa, L. Sun, D. Volkmer and P. Van Der Voort, *Dalton Trans.*, 2013, **42**, 4730; (*b*) M. Lammert, S. Bernt, F. Vermoortele, D. E. De Vos and N. Stock, *Inorg. Chem.*, 2013, **52**, 8521; (*c*) M. L. Foo, S. Horike, T. Fukushima, Y. Hijikata, Y. Kubota, M. Takata and S. Kitagawa, *Dalton Trans.*, 2012, **41**, 13791; (*d*) B. Li, Y. Zhang, D. Ma, L. Li, G. Li, G. Li, Z. Shi and S. Feng, *Chem. Commun.*, 2012, **48**, 6151.

9 G. Chang, M. Huang, Y. Su, H. Xing, B. Su, Z. Zhang, Q. Yang, Y. Yang, Q. Ren, Z. Bao and B. Chen, *Chem. Commun.*, 2015, **51**, 2859.

10 (*a*) D. F. Othmer, K. Kon and T. Igarashi, *Ind. Eng. Chem.*, 1948, **48**, 1258; (*b*) V. H. Agreda, *Acetic Acid and its Derivatives*, CRC Press, 1992.

11 R. Jira, *Angew. Chem., Int. Ed.*, 2009, **48**, 9034.

12 (*a*) S. Liang, J. Jasinski, G. B. Hammond and B. Xu, *Org. Lett.*, 2015, **17**, 162; (*b*) J. Cordon, G. Jimenez-Oses, J. M. Lopez-de-Luzuriaga, M. Monge, M. E. Olmos and D. Pascual, *Organometallics*, 2014, **33**, 3823; (*c*) L. Li, M. Zeng and S. B. Herzon, *Angew. Chem., Int. Ed.*, 2014, **53**, 7892; (*d*) S. Wang, C. Miao, W. Wang, Z. Lei and W. Sun, *ChemCatChem*, 2014, **6**, 1612; (*e*) W. Wang, A. Zheng, P. Zhao, C. Xia and F. Li, *ACS Catal.*, 2014, **4**, 321; (*f*) W. E. Brenzovich, Jr., *Angew. Chem., Int. Ed.*, 2012, **51**, 8933; (*g*) F.-X. Zhu, W. Wang and H.-X. Li, *J. Am. Chem. Soc.*, 2011, **133**, 11632.

